*Evolution*, 2025, **79(7)**, 1310–1321
https://doi.org/10.1093/evolut/qpaf077
Advance access publication 23 April 2025
**Original Article**

# Selection on a single locus drives plumage differentiation in the Rufous-collared Sparrow (*Zonotrichia capensis*)

**Pablo D. Lavinia[1,2,*], Leonardo Campagna[3,4], Martín Carboni[5], Ana S. Barreira[5], Stephen C. Lougheed[6], Pablo L. Tubaro[5], Darío A. Lijtmaer[5]**

[1]Universidad Nacional de Río Negro, Laboratorio de Investigación y Conservación de la Biodiversidad (UNRN–InCoBIO), Sede Atlántica, Viedma, Río Negro, Argentina
[2]Universidad Nacional de Río Negro, CIT Río Negro (UNRN–CONICET), Sede Atlántica, Viedma, Río Negro, Argentina
[3]Fuller Evolutionary Biology Program, Cornell Lab of Ornithology, Cornell University, Ithaca, NY, United States
[4]Department of Ecology and Evolutionary Biology, Cornell University, Ithaca, NY, United States
[5]División Ornitología, Museo Argentino de Ciencias Naturales "Bernardino Rivadavia" (MACN–CONICET), Ciudad Autónoma de Buenos Aires, Buenos Aires, Argentina
[6]Department of Biology, Queen's University, Kingston, Ontario, Canada

[*]Corresponding author: Universidad Nacional de Río Negro, Laboratorio de Investigación y Conservación de la Biodiversidad (UNRN–InCoBIO), Sede Atlántica, RP NRO. 1 Y Rotonda Cooperación S/N, CP 8500, Viedma, Río Negro, Argentina. Email: pablo.lavinia@conicet.gov.ar

## Abstract

The Rufous-collared Sparrow (*Zonotrichia capensis*) shows phenotypic variation throughout its distribution. In particular, the Patagonian subspecies *Z. c. australis* is strikingly distinct from all other subspecies, lacking the black crown stripes that characterize the species, with a uniformly grey head and overall paler plumage. We sequenced whole genomes of 18 individuals (9 *Z. c. australis* and 9 from other subspecies from northern Argentina) to explore the genomic basis of these color differences and to investigate how they may have evolved. We detected a single ~465-kb divergence peak on chromosome 5 that contrasted with a background of low genomic differentiation and contains the suppression of tumorigenicity 5 (ST5) gene. ST5 regulates RAB9A, which is required for melanosome biogenesis and melanocyte pigmentation in mammals, making it a strong candidate gene for the melanic plumage polymorphism within *Z. capensis*. This genomic island of differentiation may have emerged because of selection acting on allopatric populations or against gene flow on populations in physical and genetic contact. Mitochondrial DNA indicated that *Z. c. australis* diverged from other subspecies ~400,000 years ago, suggesting a putative role of Pleistocene glaciations. Phenotypic differences are consistent with Gloger's rule, which predicts lighter-colored individuals in colder and drier climates like that of Patagonia.

**Keywords:** coloration, DENND2B/ST5, glacial cycles, Gloger's rule, melanin, subspecies

## Introduction

Widespread species offer the possibility of investigating the interplay among evolutionary processes across different spatiotemporal scales, as distinct populations will experience different environments and demographic histories that promote diversification over hundreds to even millions of years (Bukowski et al., 2024; Klicka et al., 2023; Lavinia et al., 2015). This results in naturally occurring phenotypic polymorphisms that are often decoupled from intraspecific phylogeographic patterns, especially at shallow levels of genomic divergence, since the latter are shaped by genome-wide genetic variation presumed to evolve in a neutral or nearly neutral fashion (Winker, 2009; Zamudio et al., 2016). In contrast, fitness-related phenotypic traits may evolve rapidly due to selection on a smaller number of loci that respond to changes in local environmental conditions, and identifying the genetic basis and the underlying molecular mechanisms shaping such traits is key to understanding adaptation, diversification, and the evolution of new species (Campagna & Toews, 2022; Cuthill et al., 2017; Hill, 2006; Hubbard et al., 2010; Lawson & Petren, 2017).

Plumage coloration is an ecologically and evolutionary significant trait for birds, playing a major role in mate choice, the establishment of reproductive isolation, and the onset of speciation (Delhey et al., 2023; Hill, 2006; Mason & Bowie, 2020; Orteu & Jiggins, 2020; Price, 2008; Turbek et al., 2021; Wang et al., 2020). Over the last decade, researchers have leveraged advances in genome sequencing methods to increase our knowledge and understanding of the genomic regions and molecular processes responsible for the evolution of color-related traits in non-model organisms, and more specifically the origins and maintenance of melanin- (browns, greys, blacks, and dark reds) and carotenoid- (bright yellows, oranges, and reds) based coloration (Campagna & Toews, 2022; Funk & Taylor, 2019; Orteu & Jiggins, 2020). Biological systems with low levels of background genome-wide differentiation, but with clear coloration differences, such as rapid radiations and hybrid

Received January 13, 2025; revisions received March 19, 2025; accepted April 21, 2025

Associate Editor: Claire Mérot; Handling Editor: Hélène Morlon

zones, have been particularly fruitful for the identification of divergent genomic regions that relate to a plumage trait and contain candidate genes and regulatory elements for color production (Estalles et al., 2022; Funk & Taylor, 2019; Turbek et al., 2021; Wang et al., 2020). Conspecific populations or subspecies differing in coloration are also suitable for this approach, constituting great models for understanding the forces that shape intraspecific evolutionary trajectories and that might facilitate the emergence of new species. However, studies below the species level have been comparatively scarce (Abolins-Abols et al., 2018; Aguillon et al., 2021; Bourgeois et al., 2017; Brelsford et al., 2017).

The Rufous-collared Sparrow (*Zonotrichia capensis*) is a ubiquitous passerine ranging from Chiapas (Mexico) to Cape Horn (Chile), absent only in continuous closed forest habitats like Amazonia (Figure 1A; BirdLife International, 2024). Over this vast range, the species shows variation in morphology, plumage coloration, and behavior (Handford, 1983; Rising & Jaramillo, 2020). However, phenotypic variation does not match subspecies designations (Chapman, 1940; Handford, 1985; Nottebohm, 1969, 1975) or genetic lineages (Campagna et al., 2014; Lougheed et al., 2013). Regarding the latter, previous studies show that three mitochondrial lineages exist throughout the *Z. capensis* range. These originated during the Pleistocene as the result of historical isolation and the southward colonization of South America from a probable Central American origin (Campagna et al., 2014; Lougheed et al., 2013). An exception to this overall mismatch between subspecific designations and phenotypic differentiation is the southernmost subspecies, *Z. c. australis* from Patagonia, which shows striking differentiation from all other subspecies because it lacks the lateral black crown stripes characteristic of the species, resulting in a uniformly grey head or one with only

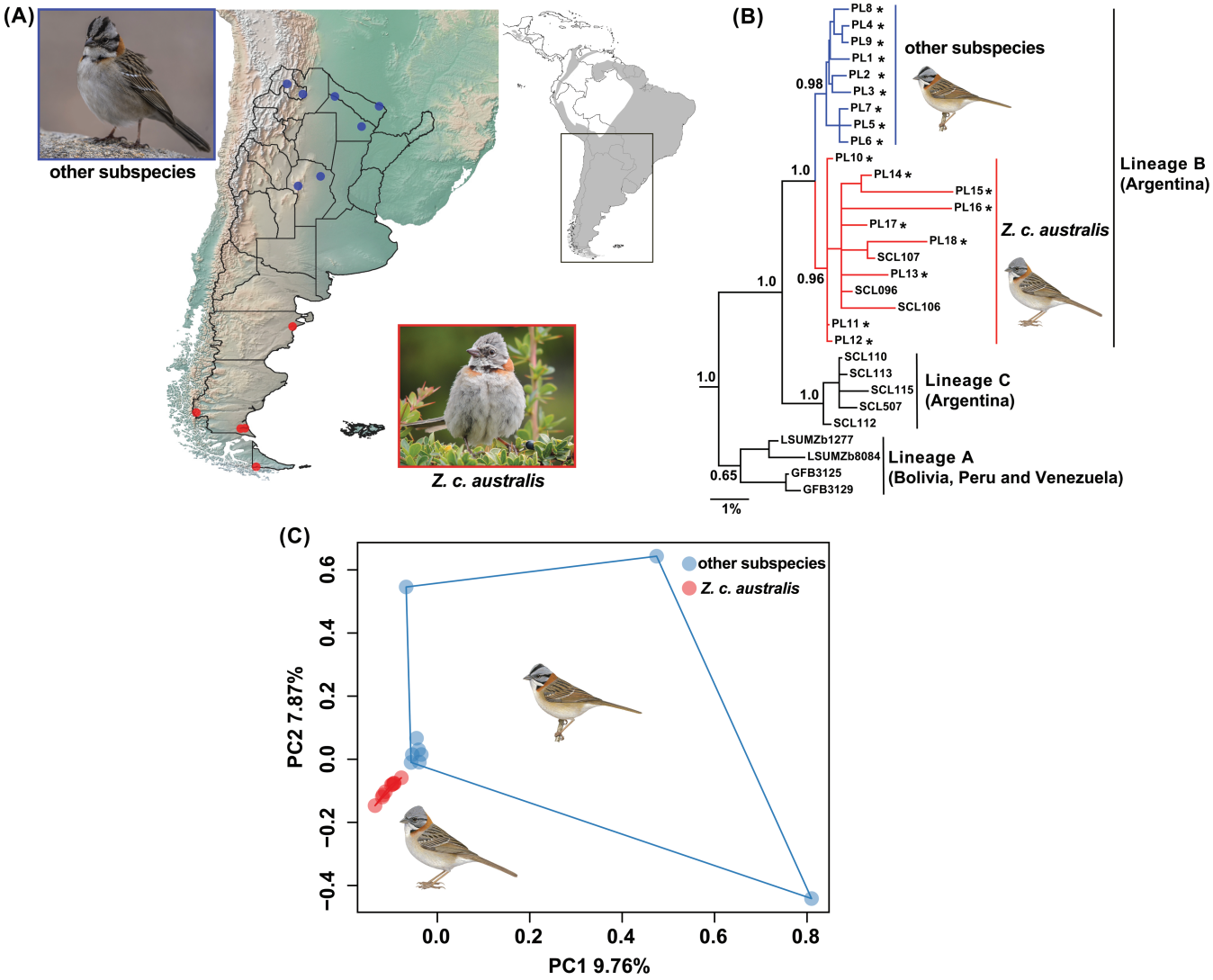


**Figure 1.** (A) Geographic origin of the individuals sequenced in this study representing the grey-headed subspecies *Z. c. australis* (in red) and the other subspecies that possess the black crown stripes (in blue), depicted over an elevation map of southern South America with Argentinian provinces delimited. The inset in the upper right shows the continental distribution of *Z. capensis* in grey (BirdLife International, 2024). Photo credits: Pablo D. Lavinia (*Z. c. australis*) and Agustín I. Casale (other subspecies). (B) Bayesian 50% majority rule consensus tree inferred from the analysis of mitochondrial DNA. Numbers above or below the branches indicate node support. Lineage names are based on Lougheed et al. (2013), and individuals sequenced for this project (PL1–PL9: other subspecies; PL10–PL18: *Z. c. australis*; Supplementary Table S1) are denoted by an asterisk; all other sequences were obtained from Lougheed et al. (2013). Outgroups are not shown for simplicity. (C) Principal component analysis (PCA) based on ~ 11 million nuclear SNPs. Bird illustrations are from del Hoyo et al. (2018).

subtle traces of black (Figure 1A). In fact, all other black plumage patches are paler or less prominent in this subspecies. *Z. c. australis* is also a long-distance latitudinal migrant, with southern populations migrating as far north as southern Bolivia in the winter (Chapman, 1940; Handford, 1985; Lisovski et al., 2025). Lastly, *Z. c. australis* is also genetically differentiated from the rest of the species. However, genetic divergence is not particularly deep, as *Z. c. australis* forms a subclade within the species most widespread mitochondrial lineage (lineage B *sensu* Lougheed et al., 2013) that also includes another seven subspecies that do possess the black crown stripes.

Here, we take advantage of the combination of low levels of genomic divergence and clear plumage pattern differentiation between the gray-headed *Z. c. australis* and other subspecies that show the black crown stripes, and use whole genomes to investigate the genomic basis underlying color differences. We also explore how these pigmentation differences may have evolved in the context of the diversification history of Patagonian populations. Our results reveal a new candidate gene underpinning the melanic plumage polymorphism within *Z. capensis* and suggest a putative role of Pleistocene glaciations in the evolutionary history of *Z. c. australis* in southern South America.

## Materials and methods

### Sampling and sequencing

We performed whole genome resequencing of nine representatives of the grey-headed *Z. c. australis* from Argentinian Patagonia and nine individuals from northern Argentina that possess the typical black crown stripes (Figure 1A, Supplementary Table S1). All samples were obtained by the authors. Because all subspecies other than *Z. c. australis* do exhibit the characteristic black head marks (Chapman, 1940), all individuals from northern Argentina were grouped and analyzed together (hereafter referred to as "other subspecies"). We selected the 18 individuals to be members of the mitochondrial lineage B based on Lougheed et al. (2013) and Campagna et al. (2014), and intentionally avoided a contact zone in northern Patagonia and central Argentina where some individuals show intermediate phenotypes. Therefore, here we focused on the comparison between two clearly distinct morphs (grey head represented by *Z. c. australis* vs. black crown stripes represented by all other subspecies), enabling a better identification of the genomic regions underlying plumage coloration in this system.

Total genomic DNA was extracted using a standard phenol/chloroform protocol followed by an ethanol precipitation and magnetic bead cleanup. We used 200 ng of extracted DNA for each sample to generate individual barcoded libraries using the TruSeq Nano DNA kit protocol (Illumina), with an insert size of 550 bp, and following the manufacturer's protocol. All individuals were pooled and sequenced (2 × 150 paired end) on an Illumina NextSeq 500 lane at the Cornell Institute for Biotechnology core facility.

### Filtering, alignment, and variant discovery

We obtained a total of over 714 million raw paired-end reads, with a length of 151 bp, representing a mean expected per-individual coverage of 5.7× ± 1.9× (range of 2.6×–9.1×; Supplementary Table S2) based on the reference genome size of ~1.05 Gbp (Tuttle et al., 2016). We assessed the quality of individual libraries with fastqc 0.11.7 (www.bioinformatics.babraham.ac.uk/projects/fastqc). Adapter removal, quality filtering, and sequence trimming were performed with AdapterRemoval 2.2.2 (Schubert et al., 2016), allowing a minimum Phred quality score of 10 and merging overlapping paired-end reads. After quality filtering, we retained 663 million reads with an average expected per-individual coverage of 5.3× ± 1.8× (range 2.2×–8.7×; Supplementary Table S2). Filtered reads were aligned to the genome of the White-throated Sparrow (*Zonotrichia albicollis;* GenBank assembly accession: GCA_000385455.1; Tuttle et al., 2016) with the very sensitive local option implemented in Bowtie 2 2.3.4.1 (Langmead & Salzberg, 2012). We used Qualimap 2.2.1 (García-Alcalde et al., 2012) to obtain alignment statistics. The average alignment rate across all samples was 92.8% ± 0.90% (range 90.9%–94.0%) leading to a final average coverage of 4.9× ± 1.7× (range 2.0×–8.1×, Supplementary Table S2).

SAM files resulting from alignment were converted to BAM format and then sorted and indexed using SAMtools 1.9 (Li et al., 2009). We used Picard Tools 2.8.2 (https://broadinstitute.github.io/picard/) to mark PCR duplicates first and to fix mate pairs after realigning around indels with GATK 3.8.1 (McKenna et al., 2010). Variant discovery and genotyping for the 18 individuals were performed with GATK. We first used the HaplotypeCaller module to produce individual genomic variant call files for each sample under default settings, and subsequently used the GenotypeGVCFs module to obtain a single variant file for the entire dataset. We retained 25,335,830 single-nucleotide polymorphisms (SNPs) after filtering out variants that were flagged by the following hard filters: QD < 2, FS > 60.0, MQ < 40.0, MQRankSum < −12.5, and ReadPosRankSum < −8.0. Finally, we used VCFtools 0.1.15 (Danecek et al., 2011) to retain only biallelic variant sites with less than 10% missing data, at least 2% minimum allele frequency, and a depth of coverage between 2× and 50×. This resulted in a dataset of 10,798,248 SNPs with an average depth of coverage across sites per individual of 4.4× ± 1.5× (range 2.0×–7.1×) and an average of 2.7% ± 3.2% of missing data per individual (range 0.1%–13.5%; Supplementary Table S2).

### Mitochondrial genomes and phylogenetic trees

We used the raw paired-end reads with only the adapters removed to extract and assemble mitochondrial genomes with NOVOPlasty (Dierckxsens et al., 2017), and complemented this with MITObim (Hahn et al., 2013) as needed. For NOVOPlasty, we used the cytochrome *c* oxidase subunit I (COI) sequence of one of our *Z. capensis* samples (MACN-Or-ct 1093; GenBank accession number: FJ028602.1) as a seed and the partial mitochondrial genome of the White-crowned Sparrow (*Zonotrichia leucophrys*) as reference (GenBank accession number: FJ236292.1). MITObim was run for up to 40 iterations, under the quick option and using *Z. leucophrys* genome as a template. After visually inspecting, manually editing, and aligning contigs in MEGA (Tamura et al., 2011), we were able to recover between ~10,000 and ~17,000 bp of the mitochondrial genomes of all 18 individuals that were used for downstream analyses. Per-site nucleotide diversity ($\pi$) within groups and mean uncorrected genetic distances (*p*-distances) between them were estimated in DnaSP (Librado & Rozas, 2009) and MEGA, respectively.

To increase our sample size for phylogenetic analyses, we mined from GenBank mitochondrial data previously generated by Lougheed et al. (2013). Specifically, we included

sequences from four mitochondrial loci (control region, 16 S rDNA, NADH dehydrogenase subunit 2, and COI) for individuals representing the three lineages (A, B, and C *sensu* Lougheed et al., 2013) of *Z. capensis*. We also included sequence data from its congeners *Z. albicollis* and the Harris' Sparrow (*Zonotrichia querula*) to be used as outgroups together with *Z. leucophrys* (Supplementary Table S3). Gene trees were inferred with the Bayesian and Maximum Likelihood (ML) algorithms using MrBayes 3.2.2 (Ronquist et al., 2012) and RAxML 8.1.22 (Stamatakis, 2014), respectively. Bayesian analysis consisted of two independent runs of 15 million generations under the HKY + I + G model of nucleotide substitution selected using the Bayesian information criterion (BIC) as implemented in jModelTest 2.1.1 (Darriba et al., 2012), with default priors and sampling trees every 100 generations. The average standard deviation of split frequencies between runs was < 0.01, indicating convergence. We used Tracer 1.7.2 (Rambaut & Drummond, 2007) to confirm that both runs reached stationarity and that we had a good sample of the posterior probability distribution. After discarding the first 25% of sampled trees as burn-in, the remaining 112,500 topologies of each run were combined to generate a 50% majority rule consensus tree. The ML tree was obtained through 100 independent searches under the GTRGAMMA model of evolution. Node support values were generated with 1,000 rapid bootstrap pseudoreplicates and printed on the best-scoring ML tree.

## Population genomic analyses

We first assessed individual clustering with a principal component analysis (PCA) based on the ~11 million genome-wide SNPs using the R 3.5 (R team, 2018) package SNPRelate 1.16 (Zheng et al., 2012). We then created a thinned dataset of 41,778 SNPs with VCFtools by retaining one SNP per 25,000 bp to avoid using SNPs in high linkage disequilibrium, and used it to assess population structure and admixture. We used STRUCTURE 2.3.4 (Pritchard et al., 2000) under the admixture ancestry model and with correlated allele frequencies to run 10 replicates for each value of $K = 1$–$5$. Each run consisted of 500,000 generations following a burn-in period of 200,000 generations. We determined the most likely $K$ value with the $\Delta K$ method described by Evanno et al. (2005) as implemented in Structure Harvester (Earl & VonHoldt, 2012). Runs for the optimal $K$ value were combined in CLUMPP 1.1.2 (Jakobsson & Rosenberg, 2007) and plotted with Structure plot 2.0 (Ramasamy et al., 2014). Considering that Campagna et al. (2014) did not find phylogeographic structure within Argentina in *Z. capensis* and that Evanno's method cannot indicate $K = 1$ as most likely, we also assessed population structure using the model-free *K-means* clustering algorithm as implemented in the R package adegenet 2.1.10 (Jombart, 2008). We ran the "find.clusters" function to evaluate up to $K = 10$, performing 1 million iterations, starting from 1,000 randomly chosen centroids per $K$ value, and selecting the optimal number of genetic clusters using the lowest BIC value.

Genome-wide nucleotide diversity within each group ($\pi_w$) was estimated for nonoverlapping windows of size 15,000 nucleotides including both variant and invariant sites that passed the quality filters (see below) and using the "popgenWindows.py" python script developed by S. H. Martin (downloaded from: https://github.com/simonhmartin/genomics_general/blob/master/popgenWindows.py)

## Location of divergence peaks and candidate gene identification

We looked for regions of elevated differentiation compared with a background of low genomic differentiation (i.e., divergence peaks) by scanning the genome in nonoverlapping windows of 15,000 bp and estimating pairwise $F_{ST}$ (Weir & Cockerham, 1984) values between *Z. c. australis* and the other subspecies with VCFtools. We discarded regions with less than two windows and windows with less than 10 SNPs and visualized $F_{ST}$ variation across the genome with a Manhattan plot built with the package qqman 0.1.4 (Turner, 2018) in R. We took a conservative approach and considered a genomic region as an outlier when its mean $F_{ST}$ fell 10 *SD*s above the average $F_{ST}$ across the genome, which corresponded to an $F_{ST}$ value ≥ 0.2, and it had at least one SNP with an individual $F_{ST}$ value ≥ 0.8. Finally, we focused on scaffolds of interest and calculated $F_{ST}$ values for individual SNPs using VCFtools.

To search for genes of interest within or near the outlier regions identified, we used the NCBI's Genome Data Viewer (Rangwala et al., 2021) to explore the reference scaffolds containing those areas in the annotated genome of *Z. albicollis*. We then used NCBI's BLAST (Johnson et al., 2008) to align the reference scaffolds of *Z. albicollis* to the Zebra finch (*Taenopygia guttata*) genome (GenBank assembly accession: GCF_003957565.2) and map the chromosomal location of the divergence peaks.

## Emergence of the genomic island of differentiation

Because $F_{ST}$ is a measure of population differentiation relative to total genetic diversity, it can be elevated either because divergence between populations is also high or because intraspecific variation in one or both populations is low. Basically, these two scenarios differ in the relative contributions of gene flow and geographic isolation and in the type of selection acting on a certain genomic region. Therefore, to better understand the processes shaping the identified divergence peak, we compared $F_{ST}$ to between-group absolute nucleotide differentiation ($\pi_B$ also known as $D_{xy}$) and within-group nucleotide diversity ($\pi_w$) across the entire scaffold of interest. In a "divergence-with-gene-flow" model, selection at a locus acts against gene flow between two differentiating populations that are in physical and genetic contact. In this context, $\pi_B$ is expected to be higher in regions of high $F_{ST}$ than in those of low $F_{ST}$ as the former cause reproductive isolation and have therefore reduced gene flow, while the latter can move more freely between populations. In contrast, under the "selection-in-allopatry" model, $\pi_w$ is predicted to be low in regions of high $F_{ST}$ due to negative (background) or positive (directional) selection acting on one or both geographically isolated populations. Under pure selection-in-allopatry, $\pi_B$ should not be different on average between regions with high and low $F_{ST}$ (Cruickshank & Hahn, 2014; Han et al., 2017; Irwin et al., 2016, 2018).

$F_{ST}$ was estimated based only on variant sites (SNPs), while $\pi_B$ and $\pi_w$ were calculated using all sites (i.e., variant and invariant). To obtain $\pi_B$ and $\pi_w$, we first used the "allSites" option of GATK's GenotypeGVCFs module to obtain a single file containing both variant and invariant positions for the entire dataset, and then followed the methods and scripts developed by Irwin et al. (2016, 2018). We removed indels with VCFtools and then applied the same hard filters described above with GATK, and used the "vcf2minmq.pl"

perl script to remove positions with MQ < 40 but retaining sites without mapping quality (MQ) information, like invariant sites. We used VCFtools to filter out sites with more than 10% missing data and a mean depth of coverage smaller than 2× or greater than 50×. All $F_{ST}$, $\pi_B$, and $\pi_w$ values were calculated on a per-site basis and then summarized over nonoverlapping windows of size 15,000 nucleotides to avoid any bias in the statistics due to different sample sizes of sites within each window. Windowed $\pi_B$ and $\pi_w$ were estimated as the mean of the per-nucleotide values, while $F_{ST}$ for each window was estimated following Weir and Cockerham (1984) calculations (but see Irwin et al., 2018, and their custom scripts for more details). Lastly, we also used VCFtools to estimate Tajima's *D* for nonoverlapping windows of 15,000 bp based only on SNPs and explored the variation of this statistic across scaffold 42.

### Genomic differentiation at other candidate coloration loci

We assessed whether other genomic regions already reported to be associated with plumage coloration show divergence between *Z. c. australis* and the other subspecies. We looked at 17 genomic regions that have been proposed in the literature as candidate loci for color variation in general and melanic plumage polymorphism in particular (Funk & Taylor, 2019; Orteu & Jiggins, 2020). For each region of interest, we calculated mean $F_{ST}$ values between *Z. c. australis* and the other subspecies for (a) the complete scaffold that contained that locus based on nonoverlapping 15,000 bp windows and (b) inside and outside the focal locus and 100 kb around it based on individual SNPs. We compared the $F_{ST}$ variation observed at all levels and loci to that found at the divergence peak we discovered between *Z. c. australis* and the other subspecies.

## Results

The gene trees based on mitochondrial DNA sequences confirmed that all individuals sampled for this study belong to the same lineage (lineage B *sensu* Lougheed et al., 2013), which was recovered as a monophyletic group with high-to-maximum node support (Figure 1B, Supplementary Figure S1A). Mean uncorrected genetic distance between the grey-headed *Z. c. australis* and other subspecies showing the black crown stripes was 0.81% ± 0.39%. All the individuals from northern Argentina (the "other subspecies" group) were recovered as a monophyletic group with high node support. *Z. c. australis* formed a monophyletic clade with near-maximum support in the Bayesian tree (Figure 1B), but showed intermediate-to-low support in the ML topology (Supplementary Figure S1A). Nucleotide diversity was markedly higher in *Z. c. australis* ($\pi$ = 0.0088) versus the other subspecies ($\pi$ = 0.0031).

Genome-wide differentiation between *Z. c. australis* and the other subspecies based on ~11 million nuclear SNPs was low ($F_{ST}$ = 0.015 ± 0.018). Accordingly, the PCA showed a shallow separation between the two groups (Figure 1C), yet tight clustering of the *Z. c. australis* individuals. Genomic nucleotide diversity within *Z. c. australis* ($\pi$ = 0.0023) was similar to that within the other subspecies group ($\pi$ = 0.0027), contrasting with the mitochondrial DNA. The assessment of genetic population structure produced congruent results between the outputs from STRUCTURE and the *K-means* algorithms, implying that the most likely number of genetic clusters for all the samples in this study was one (Supplementary Figure S1B–E).

Genomic scans revealed a divergence peak on scaffold 42 that contrasts with the background of low genomic differentiation between *Z. c. australis* and the other sampled subspecies (Figure 2A). Differentiation at this ~465-kb region was markedly higher ($F_{ST}$ = 0.31 ± 0.09 based on 951 SNPs from outlier 15-kb windows only and $F_{ST}$ = 0.18 ± 0.13 based on 2,728 SNPs from the entire divergent region) than that calculated from the entire dataset of ~11 million SNPs ($F_{ST}$ = 0.015 ± 0.018), showing clear differentiation between *Z. c. australis* and all other individuals (Figure 2B). Moreover, this genomic island of differentiation contains 90% of outlier SNPs ($F_{ST} \geq 0.8$) and virtually all fixed differences (51/53 SNPs with an $F_{ST}$ = 1) that are located across all the 15-kb outlier windows detected in our study (Figure 2A). This peak also comprises 25% of the total 248 fixed SNPs scattered across the entire genome. Finally, based on the annotated genomes of the White-throated sparrow (*Z. albicollis*) and the Zebra finch (*T. guttata*), we mapped scaffold 42 to chromosome 5 and found that the outlier SNPs were located mainly within and downstream of the suppression of tumorigenicity 5 (ST5) gene (Figure 2C). Around 98% of outlier SNPs in the divergence peak were in noncoding regions. One outlier SNP ($F_{ST}$ = 0.87) out of 149 found within ST5 was in a coding region (exon). This variant led to a nonsynonymous *Ala349Gly* change in most individuals that possess black crown stripes (i.e., those that were not *Z. c. australis* individuals).

We found a clear decrease in within-group-diversity ($\pi_w$) inside and around the divergence peak in both groups, being this even more evident within *Z. c. australis* (Figure 3, Supplementary Figure S2, Supplementary Table S5). Concordantly, within-group variation across the entire scaffold 42 was lower in *Z. c. australis* ($\pi_w$ = 0.0017) than in the other individuals from northern Argentina ($\pi_w$ = 0.0022). In contrast, absolute nucleotide differentiation ($\pi_B$) between *Z. c. australis* and the other subspecies fluctuated across scaffold 42, without a clear trend in comparison to that observed for $\pi_w$ (Figure 3). In fact, $\pi_B$ was not different on average between regions with high and low $F_{ST}$ (Supplementary Figure S2, Supplementary Table S5). There is, however, an increase in $\pi_B$ in the region of high relative differentiation (i.e., the $F_{ST}$ peak), which was relatively clearer when looking at the per-nucleotide statistics (Supplementary Figure S3). Values of Tajima's *D* were mostly negative or close to zero across the entire scaffold, with no particular pattern in or around the divergence peak (Supplementary Figure S4).

Finally, we assessed divergence in greater detail between *Z. c. australis* and the other subspecies at 17 genomic regions that contained over 20 coloration candidate genes previously reported. Overall, differentiation at these regions is comparable to that estimated for the entire genome, and around one order of magnitude lower than that registered at the divergence peak on scaffold 42 (Supplementary Table S4). Furthermore, mean $F_{ST}$ values inside and around each focal locus were similar or even lower than those observed outside the loci and across the entire scaffold (Supplementary Table S4). Indeed, we did not find 15-kb outlier windows in any of these scaffolds, nor were these coloration genes found in outlier windows, and with few exceptions, no outlier SNPs ($F_{ST} \geq 0.8$) were found inside or proximate to these loci (Supplementary Table S4).

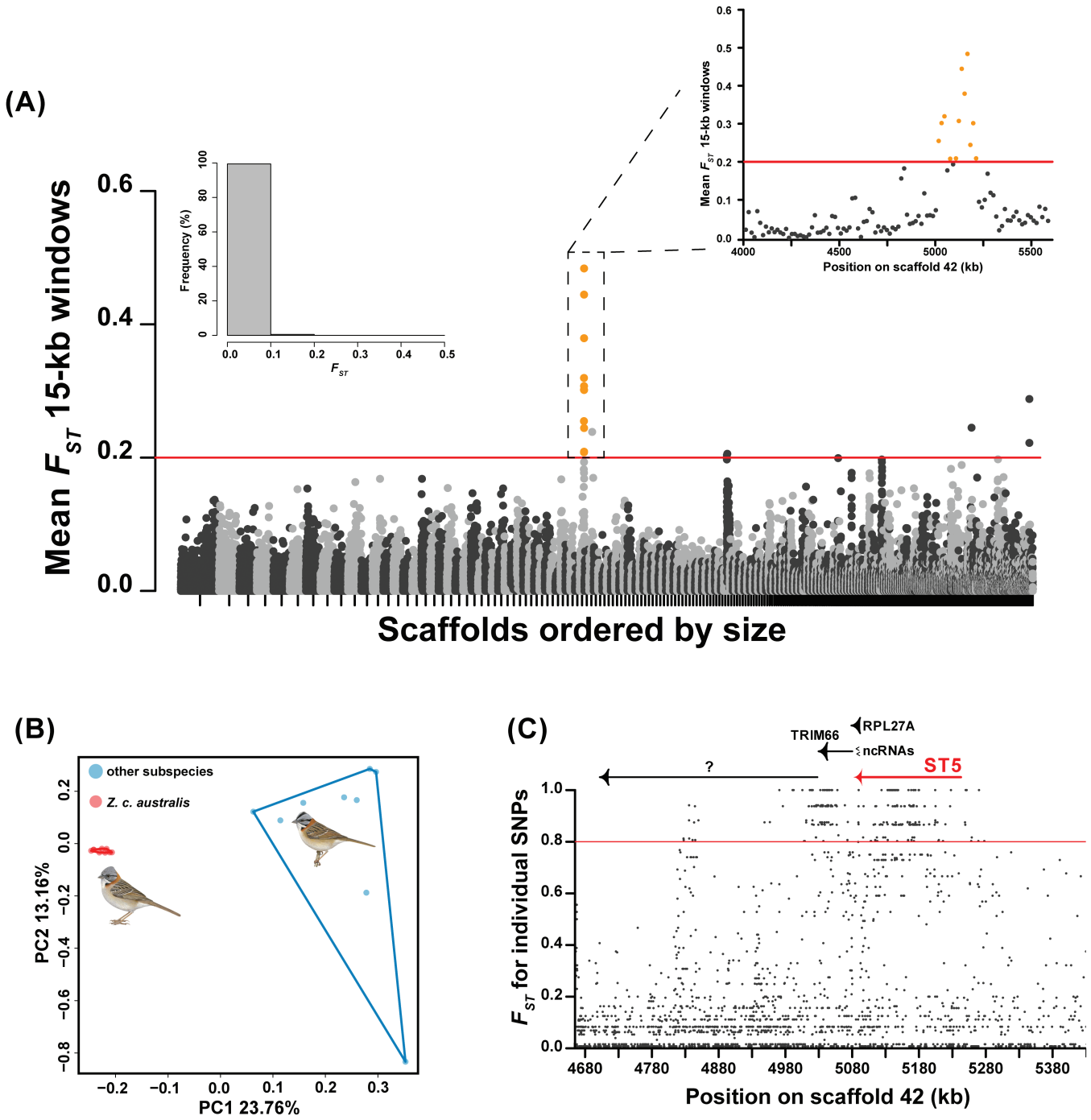


**Figure 2.** (A) Manhattan plot for the comparison between *Z. c. australis* and the other subspecies. Circles correspond to mean $F_{ST}$ values between groups for nonoverlapping 15-kb windows. Scaffolds are sorted by decreasing size and indicated by alternating black and grey colors. The red line at $F_{ST} = 0.2$ indicates the threshold used for the identification of outlier windows. Dots highlighted in orange are 15-kb divergent windows located in the divergence peak on scaffold 42. The inset on the upper right shows a zoom of scaffold 42, giving a better look at the divergence peak. The histogram on the upper left shows the frequency distribution of windowed $F_{ST}$ values across the entire genome. (B) PCA derived from the analysis of 2,728 SNPs from the divergence peak on scaffold 42. (C) $F_{ST}$ and location of individual SNPs within the peak plus 150 kb to both sides. The red line at $F_{ST} = 0.8$ indicates the threshold used for the identification of outlier individual SNPs. Arrows indicate the size and orientation of the different genes, uncharacterized loci (?) and noncoding RNAs (ncRNAs) annotated within the region. ST5 is highlighted due to its involvement in the production of melanin-based coloration.

## Discussion

Previous studies of *Z. capensis* based on Sanger-sequenced mitochondrial and nuclear markers suggested a rapid diversification of the species in the Pleistocene during its colonization of South America from a probable Central American origin (Lougheed et al., 2013). This corresponded to notable mitochondrial divergence among three main mitochondrial lineages that contrasted with a lack of nuclear genetic discontinuities, especially in southern South America. Overlying this, the species shows phenotypic and behavioral variation

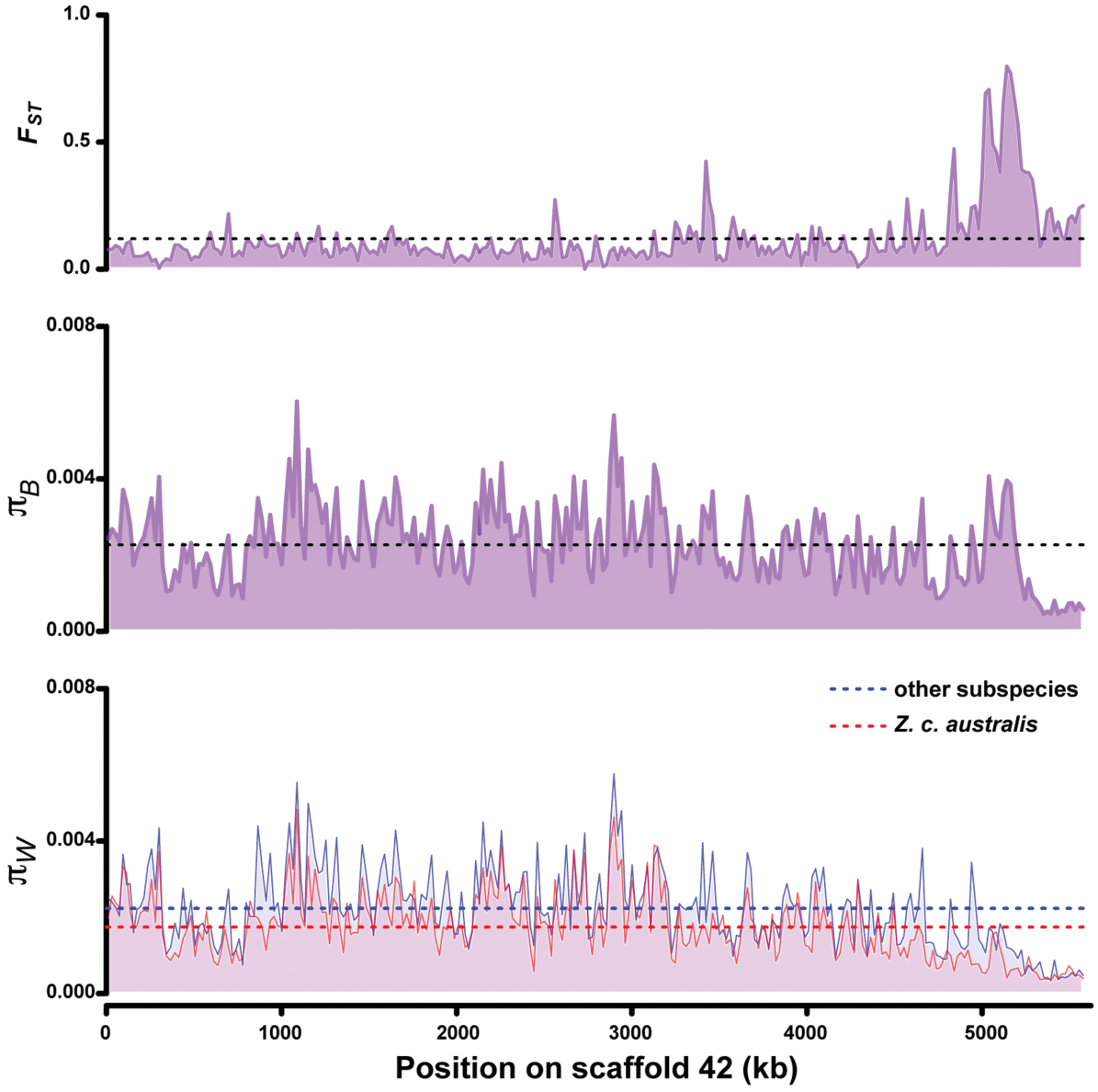


**Figure 3.** Genomic patterns of nucleotide variation across scaffold 42. Graphs show windowed relative differentiation ($F_{ST}$, top), absolute divergence ($\pi_B$, middle) between *Z. c. australis* and the other subspecies, and within-group nucleotide diversity ($\pi_w$, bottom). The dashed lines indicate the overall mean value for each summary statistic across the entire scaffold.

throughout its range, which does not match phylogeographic patterns and most likely evolved relatively rapidly in recent responses to local environmental conditions (Campagna et al., 2014; Lougheed et al., 2013). The subspecies *Z. c. australis* from Patagonia is the most distinctive of all continental subspecies, lacking the black crown stripes that characterize the species and having instead a completely grey head or one with only subtle traces of black (Chapman, 1940; Handford, 1985). Using whole genome resequencing we identified a single genomic region containing a candidate gene that might underpin this striking color polymorphism and proposed an evolutionary scenario behind its emergence.

Our results confirm that genome-wide nuclear differentiation between *Z. c. australis* and an assortment of individuals representing other subspecies from northern Argentina is remarkably low, with no clear differentiation between the two groups. However, genomic scans allowed us to identify a single, ~465-kb divergence peak on chromosome 5 that clearly differentiates the grey-headed *Z. c. australis* from all other subspecies sampled here that do possess the black crown stripes. This genomic island of differentiation (Burri, 2017) contains nearly all the outlier SNPs that are present in 15-kb outlier windows and a large proportion of the relatively few fixed SNPs scattered across the entire genome. Six annotated regions were found in this island of differentiation: ST5, tripartite motif-containing protein 66 (TRIM66), ribosomal protein L27a (RPL27A), two small nucleolar noncoding RNAs (snoRNAs), and the uncharacterized locus "LOC113459224." Among these loci, ST5 (also known as DENND2B) stands out as a candidate gene for melanic plumage polymorphism within *Z. capensis*. The DENND2 family of proteins regulates RAB9A (Ras-associated protein 9A) by acting as a guanine nucleotide exchange factor (GEF) that facilitates the exchange of GDP (guanosine diphosphate) for GTP (guanosine triphosphate) on RAB9A, switching it to its active state. In mammals, active RAB9A proteins are required

for the transport of melanin-synthesizing enzymes and other proteins needed for melanosome biogenesis from recycling endosomes to melanosomes (Mahanty et al., 2016; Yoshimura et al., 2010). Melanosomes are the lysosome-related organelles within which different enzymes produce melanin, the pigment responsible for black and brown coloration. RAB9A knockdown in melanocytes results in hypopigmented melanosomes, and defects in the function or formation of melanosomes result in oculocutaneous albinism in humans and mice (Mahanty et al., 2016).

While coding mutations often result in body-wide color changes like completely melanic morphs (Uy et al., 2016), discrete or localized changes in color patterns have been associated with regulatory changes (Funk & Taylor, 2019; Orteu & Jiggins, 2020). Mutations in noncoding regions, which could contain *cis*-regulatory elements that control the expression of coloration genes, could be responsible for patch-specific changes (Estalles et al., 2022; Funk & Taylor, 2019; Orteu & Jiggins, 2020). Moreover, noncoding mutations and regulatory changes are less likely to be deleterious or have negative pleiotropic effects than coding changes, allowing a more rapid evolution of color differences (Orteu & Jiggins, 2020). Here we found that virtually all outlier SNPs were located in noncoding regions downstream and within the ST5 gene, suggesting that differences in melanin-based pigmentation between *Z. capensis* morphs could be mostly associated with differences in gene expression. However, we found one outlier SNP ($F_{ST}$ = 0.87) within an exon of ST5 that involved a nonsynonymous change, indicating that coding changes could also be contributing to plumage coloration differences to a lesser extent. Lastly, another area worth of further exploration is the potential *cis*-regulatory role of the snoRNAs found downstream of ST5, within which no outlier SNPs were found. snoRNAs are short, conserved noncoding RNAs typically encoded in introns of ribosomal protein-coding genes (RPL27A in this case) that have been traditionally associated with ribosome biogenesis. However, recent studies have shown that snoRNAs play diverse biological functions, including the modulation of gene expression via different mechanisms that still need further investigation to be fully understood (Bratkovič et al., 2020; Wajahat et al., 2021).

If ST5 is involved in melanosome biogenesis and melanin production via regulation of RAB9A, this gene (or the entire genomic region in scaffold 42) may be a large-effect locus controlling melanin-based pigmentation differences and the existence of markedly distinct morphs in *Z. capensis*. This is supported by the fact that all the other plumage coloration genes that we examined showed negligible differences between groups, similar to that found across the entire nuclear genome. Therefore, differences in ST5 expression levels could be responsible for the uniformly grey head of *Z. c. australis*, subspecies in which all other black plumage patches are also paler or less prominent in comparison to those of other subspecies (Chapman, 1940; Handford, 1985). To our knowledge, this is the first study to report an association between ST5 and plumage coloration in birds. Our findings build on those of Bourgeois et al. (2017), who found that *cis*-regulatory, noncoding mutations in a novel locus on chromosome 1 underlie the evolution of a melanin-based coloration in the Reunion Grey White-eye (*Zosterops borbonicus*). Within this single genomic region, authors identified seven candidate genes, one of which corresponded to RAB9A. As in *Z. capensis*, melanic polymorphism within *Z. borbonicus* was not associated with previously identified melanogenesis genes such as MC1R or ASIP, highlighting that there are multiple genetic pathways through which divergence in plumage color and patterns can arise in birds (Bourgeois et al., 2017; Funk & Taylor, 2019; Orteu & Jiggins, 2020).

We found that absolute areas of elevated relative differentiation ($F_{ST}$) were associated with reduced within-group diversity ($\pi_w$) in both groups, but especially in *Z. c. australis*. On the contrary, absolute differentiation ($\pi_B$) in the divergence peak is not different on average from that observed outside the peak and across the entire scaffold. This pattern fits the "selection-in-allopatry" model, which proposes that a genomic island of differentiation emerges as the result of directional or background selection acting on one or both geographically isolated populations, therefore reducing $\pi_w$ in regions of high $F_{ST}$ (Cruickshank & Hahn, 2014; Han et al., 2017; Irwin et al., 2018). Given that background selection can affect absolute differentiation, but is not expected to elevate $F_{ST}$ values between recently diverged taxa under realistic conditions (Matthey-Doret & Whitlock, 2019), the divergence peak that we found is most likely the result of positive selection. However, because we detected a relative increase in absolute differentiation inside the divergence peak when looking at the per-nucleotide statistics, we cannot fully discard the possibility of selection acting against gene flow to some extent for this genomic region (Cruickshank & Hahn, 2014; Han et al., 2017; Irwin et al., 2018). Furthermore, if divergence between *Z. c. australis* and the other subspecies is very recent, as our mitochondrial data suggests, absolute differentiation ($\pi_B$) might not be clearly elevated because sufficient time has not gone by for differences to accumulate (Riesch et al., 2017). Therefore, both models are compatible with our data and not mutually exclusive, and currently we cannot distinguish them.

Pleistocene glacial cycles had arguably a more profound impact on Patagonian biodiversity than on that of any other lowland region of the Neotropics, more similar to what has been reported in the Northern Hemisphere (Jetz et al., 2012; Lijtmaer et al., 2011; Lovette, 2005; Sérsic et al., 2011; Weir & Schluter, 2004). In fact, the direct advance of the ice sheets that descended from the Andes, which even reached the Atlantic coast in the southernmost portion of the continent (Rabassa & Coronato, 2009; Rabassa et al., 2011), promoted the isolation and diversification of local plants and vertebrates in multiple ice-free refugia throughout Patagonia (Cosacov et al., 2010; Lessa et al., 2010; Marín et al., 2013; Nuñez et al., 2011; Sánchez et al., 2024; Sérsic et al., 2011). Our mitochondrial DNA results indicated that *Z. c. australis* diverged from the other subspecies within lineage B around 400,000 years ago based on a 2.1% divergence per million years rate (Weir & Schluter, 2008), suggesting a potential role of Pleistocene glaciations in the evolution of *Z. capensis* in Patagonia. This was previously suggested by Lougheed et al. (2013) for *Z. capensis* and is also apparent in other Neotropical birds (Acosta et al., 2021; Balza et al., 2025; Bukowski et al., 2024; Kopuchian et al., 2016). One possibility is that glaciations isolated southern populations of *Z. capensis* in Patagonia, congruent with the "selection-in-allopatry" model. Under this scenario, phenotypic differences would have evolved rapidly during the period of geographic isolation, remaining to the present in spite of the resumption of gene flow with other populations after the retreat of the glacial ice sheets (Bukowski et al., 2024; Campagna et

al., 2014; Lougheed et al., 2013). However, as we mentioned above, many biogeographic models are compatible with our data, so further work with a more geographically comprehensive sampling of Patagonia is needed to distinguish among them.

Future studies should focus on northern Patagonia and central Argentina, where there is a contact zone with some individuals showing intermediate color patterns, most likely because of gene flow between *Z. c. australis* and other subspecies (possibly *Z. c. choraules* and/or *Z. c. chilensis*). Here, we intentionally avoided sampling from this transition zone to better identify candidate loci behind plumage differences. Our findings here set the stage for future research in this contact region to assess whether color differences between subspecies promote reproductive isolation and incipient speciation of *Z. c. australis* through mate choice, as it has been shown for other closely related lineages of birds (Turbek et al., 2021; Uy et al., 2018). If this is the case, we expect the divergence peak found in this study to be one of the few regions resisting gene flow between subspecies, thus constituting a genomic island of speciation (Burri, 2017).

Our results imply that the patterns of geographic variation in melanin-based coloration within *Z. capensis* are shaped by adaptive mechanisms and consistent with the expectation of Gloger's rule, one of the oldest ecogeographical rules linking coloration in endotherms with environmental variables (Rensch, 1929). Gloger's rule predicts darker colored individuals in humid, warm, and densely vegetated areas due to an increased deposition of melanin pigments, probably associated with better camouflage, photoprotection, thermoregulation, and parasite resistance (Delhey, 2017, 2019). In contrast, paler-colored individuals (i.e., less pigmented) are expected in colder and drier climates, like that of Patagonia where the grey-headed *Z. c. australis* is found. However, there remains debate on the mechanisms behind Gloger's rule. For example, Bogert's rule proposes that individuals with higher levels of melanism should be more common in colder regions since darker coloration can absorb more solar energy to warm up (Bogert, 1949; Delhey, 2018; Galván et al., 2018). Future studies should experimentally evaluate the adaptive benefits of the lighter plumage coloration of *Z. c. australis* in Patagonia (e.g., camouflage vs. thermoregulatory), disentangling the differential effects that humidity and temperature may have on plumage coloration (López-Rull et al., 2023; Rogalla et al., 2021).

## Supplementary material

Supplementary material is available online at *Evolution*.

## Data availability

Raw genomic reads as well as processed nuclear genomic and mitochondrial genetic data used for analyses are available in Dryad (https://doi.org/10.5061/dryad.dz08kps7s).

## Author contributions

P.D.L., L.C., D.A.L., and P.L.T. conceived the idea, designed the research, and acquired the funding. S.C.L., L.C., and A.S.B. contributed with samples. P.D.L. generated the genomic data, performed the bioinformatic analyses with help from L.C. and M.C., and wrote the manuscript. All authors provided feedback on the manuscript and approved the submitted version.

## Funding

This work was supported by the Consejo Nacional de Investigaciones Científicas y Técnicas (CONICET), the Agencia Nacional de Promoción de la Investigación, el Desarrollo Tecnológico y la Innovación (AGENCIA I+D+i) from Argentina, the Richard Lounsbery Foundation and the British Ornithologists' Union.

## Conflict of interest

The authors declare no conflict of interest.

## Acknowledgments

We thank members of the Ornithology Division of the MACN (especially Y. Davies and L. Barone) and other researchers who contributed with sample acquisition and processing. We also thank N. García and C. Estalles for their insights on the bioinformatic analyses, and I. Lovette and B. Butcher for their assistance generating the genomic data. We thank the various Offices of Fauna of the provinces in which field work was conducted, the National Parks Administration, and the former National Ministry of Environment and Sustainable Development from Argentina for granting all the permits and transit guides we requested for this study.

## References

Abolins-Abols, M., Kornobis, E., Ribeca, P., Wakamatsu, K., Peterson, M. P., Ketterson, E. D., & Milá, B. (2018). Differential gene regulation underlies variation in melanic plumage coloration in the dark-eyed junco (*Junco hyemalis*). *Molecular Ecology*, *27*(22), 4501–4515. https://doi.org/10.1111/mec.14878

Acosta, I., Cabanne, G. S., Noll, D., González-Acuña, D., Pliscoff, P., & Vianna, J. A. (2021). Patagonian glacial effects on the endemic Green-backed Firecrown, *Sephanoides sephaniodes* (Aves: Trochilidae): Evidence from species distribution models and molecular data. *Journal of Ornithology*, *162*(1), 289–301. https://doi.org/10.1007/s10336-020-01822-4

Aguillon, S. M., Walsh, J., & Lovette, I. J. (2021). Extensive hybridization reveals multiple coloration genes underlying a complex plumage phenotype. *Proceedings of the Royal Society B: Biological Sciences*, *288*(1943), 20201805. https://doi.org/10.1098/rspb.2020.1805

Balza, U., Lois, N. A., Harrington, K. J., León, F., Pütz, K., Raya-Rey, A., & Ceballos, S. G. (2025). Glacial history and ecological restrictions shape island-scale genetic structure and demography in the southernmost bird of prey. *Journal of Biogeography*, *52*, e15083. https://doi.org/10.1111/jbi.15083

BirdLife International. (2024, December 4). *Species factsheet: Rufous-collared Sparrow Zonotrichia capensis*. https://datazone.birdlife.org/species/factsheet/rufous-collared-sparrow-zonotrichia-capensis

Bogert, C. M. (1949). Thermoregulation in reptiles, a factor in evolution. *Evolution*, *3*(3), 195–211. https://doi.org/10.1111/j.1558-5646.1949.tb00021.x

Bourgeois, Y. X. C., Delahaie, B., Gautier, M., Lhuillier, E., Malé, P.-J. G., Bertrand, J. A. M., Cornuault, J., Wakamatsu, K., Bouchez, O., Mould, C., Bruxaux, J., Holota, H., Milá, B., & Thébaud, C. (2017). A novel locus on chromosome 1 underlies the evolution of a melanic plumage polymorphism in a wild songbird. *Royal Society Open Science*, *4*(2), 160805. https://doi.org/10.1098/rsos.160805

Bratkovič, T., Božič, J., & Rogelj, B. (2020). Functional diversity of small nucleolar RNAs. *Nucleic Acids Research*, *48*(4), 1627–1651. https://doi.org/10.1093/nar/gkz1140

Brelsford, A., Toews, D. P. L., & Irwin, D. E. (2017). Admixture mapping in a hybrid zone reveals loci associated with avian feather coloration. *Proceedings of the Royal Society B: Biological Sciences*, *284*(1866), 20171106. https://doi.org/10.1098/rspb.2017.1106

Bukowski, B., Campagna, L., Rodríguez-Cajarville, M. J., Cabanne, G. S., Tubaro, P. L., & Lijtmaer, D. A. (2024). The role of glaciations in the evolutionary history of a widely distributed Neotropical open habitat bird. *Journal of Biogeography*, *51*(2), 199–214. https://doi.org/10.1111/JBI.14738

Burri, R. (2017). Interpreting differentiation landscapes in the light of long-term linked selection. *Evolution Letters*, *1*(3), 118–131. https://doi.org/10.1002/evl3.14

Campagna, L., Kopuchian, C., Tubaro, P. L., & Lougheed, S. C. (2014). Secondary contact followed by gene flow between divergent mitochondrial lineages of a widespread Neotropical songbird (*Zonotrichia capensis*). *Biological Journal of the Linnean Society*, *111*(4), 863–868. https://doi.org/10.1111/bij.12272

Campagna, L., & Toews, D. P. L. (2022). The genomics of adaptation in birds. *Current Biology*, *32*(20), R1173–R1186. https://doi.org/10.1016/j.cub.2022.07.076

Chapman, F. M. (1940). The post-glacial history of *Zonotrichia capensis*. *American Museum of Natural History*, *77*, 381–438.

Cosacov, A., Sérsic, A. N., Sosa, V., Johnson, L. A., & Cocucci, A. A. (2010). Multiple periglacial refugia in the Patagonian steppe and post-glacial colonization of the Andes: The phylogeography of *Calceolaria polyrhiza*. *Journal of Biogeography*, *37*(8), 1463–1477. https://doi.org/10.1111/j.1365-2699.2010.02307.x

Cruickshank, T. E., & Hahn, M. W. (2014). Reanalysis suggests that genomic islands of speciation are due to reduced diversity, not reduced gene flow. *Molecular Ecology*, *23*(13), 3133–3157. https://doi.org/10.1111/mec.12796

Cuthill, I. C., Allen, W. L., Arbuckle, K., Caspers, B., Chaplin, G., Hauber, M. E., Hill, G. E., Jablonski, N. G., Jiggins, C. D., Kelber, A., Mappes, J., Marshall, J., Merrill, R., Osorio, D., Prum, R., Roberts, N. W., Roulin, A., Rowland, H. M., Sherratt, T. N., … Caro, T. (2017). The biology of color. *Science*, *357*(6350), eaan0221. https://doi.org/10.1126/science.aan0221

Danecek, P., Auton, A., Abecasis, G., Albers, C. A., Banks, E., DePristo, M. A., Handsaker, R. E., Lunter, G., Marth, G. T., Sherry, S. T., McVean, G., & Durbin, R.; 1000 Genomes Project Analysis Group (2011). The variant call format and VCFtools. *Bioinformatics*, *27*(15), 2156–2158. https://doi.org/10.1093/bioinformatics/btr330

Darriba, D., Taboada, G. L., Doallo, R., & Posada, D. (2012). jModelTest 2: More models, new heuristics and parallel computing. *Nature Methods*, *9*(8), 772. https://doi.org/10.1038/nmeth.2109

del Hoyo, J., Elliott, A., Sargatal, J., Christie, D.A. & de Juana, E. (2018). *Handbook of the birds of the world alive*. Lynx Edicions.

Delhey, K. (2017). Gloger's rule. *Current Biology*, *27*(14), R689–R691. https://doi.org/10.1016/j.cub.2017.04.031

Delhey, K. (2018). Darker where cold and wet: Australian birds follow their own version of Gloger's rule. *Ecography*, *41*(4), 673–683. https://doi.org/10.1111/ecog.03040

Delhey, K. (2019). A review of Gloger's rule, an ecogeographical rule of colour: Definitions, interpretations and evidence. *Biological Reviews of the Cambridge Philosophical Society*, *94*(4), 1294–1316. https://doi.org/10.1111/brv.12503

Delhey, K., Valcu, M., Muck, C., Dale, J., & Kempenaers, B. (2023). Evolutionary predictors of the specific colors of birds. *Proceedings of the National Academy of Sciences of the United States of America*, *120*(34), e2217692120. https://doi.org/10.1073/pnas.2217692120

Dierckxsens, N., Mardulyn, P., & Smits, G. (2017). NOVOPlasty: de novo assembly of organelle genomes from whole genome data. *Nucleic Acids Research*, *45*(4), e18–e18. https://doi.org/10.1093/nar/gkw955

Earl, D. A., & VonHoldt, B. M. (2012). STRUCTURE HARVESTER: A website and program for visualizing STRUCTURE output and implementing the Evanno method. *Conservation Genetics Resources*, *4*(2), 359–361. https://doi.org/10.1007/s12686-011-9548-7

Estalles, C., Turbek, S. P., Jose Rodriguez-Cajarville, M., Silveira, L. F., Wakamatsu, K., Ito, S., Lovette, I. J., Tubaro, P. L., Lijtmaer, D. A., & Campagna, L. (2022). Concerted variation in melanogenesis genes underlies emergent patterning of plumage in capuchino seedeaters. *Proceedings of the Royal Society B: Biological Sciences*, *289*(1966), 20212277. https://doi.org/10.1098/rspb.2021.2277

Evanno, G., Regnaut, S., & Goudet, J. (2005). Detecting the number of clusters of individuals using the software structure: A simulation study. *Molecular Ecology*, *14*(8), 2611–2620. https://doi.org/10.1111/j.1365-294X.2005.02553.x

Funk, E. R., & Taylor, S. A. (2019). High-throughput sequencing is revealing genetic associations with avian plumage color. *The Auk*, *136*(4), ukz048. https://doi.org/10.1093/auk/ukz048

Galván, I., Rodríguez-Martínez, S., & Carrascal, L. M. (2018). Dark pigmentation limits thermal niche position in birds. *Functional Ecology*, *32*, 1531–1540.

García-Alcalde, F., Okonechnikov, K., Carbonell, J., Cruz, L. M., Götz, S., Tarazona, S., Dopazo, J., Meyer, T. F., & Conesa, A. (2012). Qualimap: evaluating next-generation sequencing alignment data. *Bioinformatics*, *28*, 2678–2679.

Hahn, C., Bachmann, L., & Chevreux, B. (2013). Reconstructing mitochondrial genomes directly from genomic next-generation sequencing reads—A baiting and iterative mapping approach. *Nucleic Acids Research*, *41*(13), e129–e129. https://doi.org/10.1093/nar/gkt371

Han, F., Lamichhaney, S., Grant, B. R., Grant, P. R., Andersson, L., & Webster, M. T. (2017). Gene flow, ancient polymorphism, and ecological adaptation shape the genomic landscape of divergence among Darwin's finches. *Genome Research*, *27*(6), 1004–1015. https://doi.org/10.1101/gr.212522.116

Handford, P. (1983). Continental patterns of morphological variation in a South American Sparrow. *Evolution*, *37*(5), 920–930. https://doi.org/10.1111/j.1558-5646.1983.tb05621.x

Handford, P. (1985). Morphological relationships among subspecies of the rufous- collared sparrow, *Zonotrichia capensis*. *Canadian Journal of Zoology*, *63*(10), 2383–2388. https://doi.org/10.1139/z85-352

Hill, G.E. (2006). *Bird coloration, volume 2: Function and evolution*. Harvard University Press.

Hubbard, J. K., Uy, J. A. C., Hauber, M. E., Hoekstra, H. E., & Safran, R. J. (2010). Vertebrate pigmentation: From underlying genes to adaptive function. *Trends in Genetics*, *26*(5), 231–239. https://doi.org/10.1016/j.tig.2010.02.002

Irwin, D. E., Alcaide, M., Delmore, K. E., Irwin, J. H., & Owens, G. L. (2016). Recurrent selection explains parallel evolution of genomic regions of high relative but low absolute differentiation in a ring species. *Molecular Ecology*, *25*(18), 4488–4507. https://doi.org/10.1111/mec.13792

Irwin, D. E., Milá, B., Toews, D. P. L., Brelsford, A., Kenyon, H. L., Porter, A. N., Grossen, C., Delmore, K. E., Alcaide, M., & Irwin, J. H. (2018). A comparison of genomic islands of differentiation across three young avian species pairs. *Molecular Ecology*, *27*(23), 4839–4855. https://doi.org/10.1111/mec.14858

Jakobsson, M., & Rosenberg, N. A. (2007). CLUMPP: A cluster matching and permutation program for dealing with label switching and multimodality in analysis of population structure. *Bioinformatics*, *23*(14), 1801–1806. https://doi.org/10.1093/bioinformatics/btm233

Jetz, W., Thomas, G. H., Joy, J. B., Hartmann, K., & Mooers, A. O. (2012). The global diversity of birds in space and time. *Nature*, *491*(7424), 444–448. https://doi.org/10.1038/nature11631

Johnson, M., Zaretskaya, I., Raytselis, Y., Merezhuk, Y., McGinnis, S., & Madden, T. L. (2008). NCBI BLAST: A better web interface. *Nucleic Acids Research*, *36*(Web Server issue), W5–W9. https://doi.org/10.1093/nar/gkn201

Jombart, T. (2008). adegenet: A R package for the multivariate analysis of genetic markers. *Bioinformatics*, *24*(11), 1403–1405. https://doi.org/10.1093/bioinformatics/btn129

Klicka, J., Epperly, K., Smith, B. T., Spellman, G. M., Chaves, J. A., Escalante, P., Witt, C. C., Canales-Del-Castillo, R., & Zink, R. M. (2023). Lineage diversity in a widely distributed New World passerine bird, the House Wren. *Ornithology*, *140*(3), ukad018. https://doi.org/10.1093/ORNITHOLOGY/UKAD018

Kopuchian, C., Campagna, L., Di Giacomo, A. S., Wilson, R. E., Bulgarella, M., Petracci, P., Mazar Barnett, J., Matus, R., Blank, O., & McCracken, K. G. (2016). Demographic history inferred from genome-wide data reveals two lineages of sheldgeese endemic to a glacial refugium in the southern Atlantic. *Journal of Biogeography*, *43*(10), 1979–1989. https://doi.org/10.1111/jbi.12767

Langmead, B., & Salzberg, S. L. (2012). Fast gapped-read alignment with Bowtie 2. *Nature Methods*, *9*(4), 357–359. https://doi.org/10.1038/nmeth.1923

Lavinia, P. D., Escalante, P., García, N. C., Barreira, A. S., Trujillo-Arias, N., Tubaro, P. L., Naoki, K., Miyaki, C. Y., Santos, F. R., & Lijtmaer, D. A. (2015). Continental-scale analysis reveals deep diversification within the polytypic Red-crowned Ant Tanager (*Habia rubica*, Cardinalidae). *Molecular Phylogenetics and Evolution*, *89*, 182–193. https://doi.org/10.1016/j.ympev.2015.04.018

Lawson, L. P., & Petren, K. (2017). The adaptive genomic landscape of beak morphology in Darwin's finches. *Molecular Ecology*, *26*(19), 4978–4989. https://doi.org/10.1111/mec.14166

Lessa, E. P., D'ElÍa, G., & PardiÑas, U. F. J. (2010). Genetic footprints of late Quaternary climate change in the diversity of Patagonian-Fueguian rodents. *Molecular Ecology*, *19*(15), 3031–3037. https://doi.org/10.1111/j.1365-294X.2010.04734.x

Li, H., Handsaker, B., Wysoker, A., Fennell, T., Ruan, J., Homer, N., Marth, G., Abecasis, G., & Durbin, R.; 1000 Genome Project Data Processing Subgroup (2009). The sequence alignment/map format and SAMtools. *Bioinformatics*, *25*(16), 2078–2079. https://doi.org/10.1093/bioinformatics/btp352

Librado, P., & Rozas, J. (2009). DnaSP v5: A software for comprehensive analysis of DNA polymorphism data. *Bioinformatics*, *25*(11), 1451–1452. https://doi.org/10.1093/bioinformatics/btp187

Lijtmaer, D. A., Kerr, K. C. R., Barreira, A. S., Hebert, P. D. N., & Tubaro, P. L. (2011). DNA barcode libraries provide insight into continental patterns of avian diversification. *PLoS One*, *6*(7), e20744. https://doi.org/10.1371/journal.pone.0020744

Lisovski, S., Wingfield, J., Ramenofsky, M., Barroso, O., de Aguilar, J. R., Valeris-Chacín, C. E., Jara, R., Aguirre, F., Quilodrán, C. S., Rozzi, R., Sandvig, E., & Vásquez, R. A. (2025). Migration in Rufous-Collared Sparrows (*Zonotrichia capensis*) from the southernmost tip of America. *Austral Ecology*, *50*, e70041.

López-Rull, I., Salaberría, C., & Fargallo, J. A. (2023). Plastic plumage colouration in response to experimental humidity supports Gloger's rule. *Scientific Reports*, *13*(1), 858.

Lougheed, S. C., Campagna, L., Dávila, J. A., Tubaro, P. L., Lijtmaer, D. A., & Handford, P. (2013). Continental phylogeography of an ecologically and morphologically diverse Neotropical songbird, *Zonotrichia capensis*. *BMC Evolutionary Biology*, *13*(1), 58. https://doi.org/10.1186/1471-2148-13-58

Lovette, I. J. (2005). Glacial cycles and the tempo of avian speciation. *Trends in Ecology & Evolution*, *20*(2), 57–59. https://doi.org/10.1016/j.tree.2004.11.011

Mahanty, S., Ravichandran, K., Chitirala, P., Prabha, J., Jani, R. A., & Setty, S. R. G. (2016). Rab9A is required for delivery of cargo from recycling endosomes to melanosomes. *Pigment Cell & Melanoma Research*, *29*(1), 43–59. https://doi.org/10.1111/pcmr.12434

Marín, J. C., Varas, V., Vila, A. R., López, R., Orozco-terWengel, P., & Corti, P. (2013). Refugia in Patagonian fjords and the eastern Andes during the Last Glacial Maximum revealed by huemul (*Hippocamelus bisulcus*) phylogeographical patterns and genetic diversity. *Journal of Biogeography*, *40*(12), 2285–2298. https://doi.org/10.1111/jbi.12161

Mason, N. A., & Bowie, R. C. K. (2020). Plumage patterns: Ecological functions, evolutionary origins, and advances in quantification. *The Auk*, *137*(4), ukaa060.

Matthey-Doret, R., & Whitlock, M. C. (2019). Background selection and *FST*: Consequences for detecting local adaptation. *Molecular Ecology*, *28*(17), 3902–3914. https://doi.org/10.1111/mec.15197

McKenna, A., Hanna, M., Banks, E., Sivachenko, A., Cibulskis, K., Kernytsky, A., Garimella, K., Altshuler, D., Gabriel, S., Daly, M., & DePristo, M. A. (2010). The Genome Analysis Toolkit: A MapReduce framework for analyzing next-generation DNA sequencing data. *Genome Research*, *20*(9), 1297–1303. https://doi.org/10.1101/gr.107524.110

Nottebohm, F. (1969). The song of the chingolo, *Zonotrichia capensis*, in Argentina: Description and evaluation of a system of dialects. *The Condor*, *71*(3), 299–315. https://doi.org/10.2307/1366306

Nottebohm, F. (1975). Continental patterns of song variability in *Zonotrichia capensis*: Some possible ecological correlates. *The American Naturalist*, *109*(970), 605–624. https://doi.org/10.1086/283033

Nuñez, J. J., Wood, N. K., Rabanal, F. E., Fontanella, F. M., & Sites, J. W. (2011). Amphibian phylogeography in the Antipodes: Refugia and postglacial colonization explain mitochondrial haplotype distribution in the Patagonian frog *Eupsophus calcaratus* (Cycloramphidae). *Molecular Phylogenetics and Evolution*, *58*(2), 343–352. https://doi.org/10.1016/j.ympev.2010.11.026

Orteu, A., & Jiggins, C. D. (2020). The genomics of coloration provides insights into adaptive evolution. *Nature Reviews Genetics*, *21*(8), 461–475. https://doi.org/10.1038/s41576-020-0234-z

Price, T. (2008). *Speciation in birds* (Vol. *709*). Roberts and Company.

Pritchard, J. K., Stephens, M., & Donnelly, P. (2000). Inference of population structure using multilocus genotype data. *Genetics*, *155*(2), 945–959. https://doi.org/10.1093/genetics/155.2.945

Rabassa, J., Coronato, A., & Martínez, O. (2011). Late Cenozoic glaciations in Patagonia and Tierra del Fuego: An updated review. *Biological Journal of the Linnean Society*, *103*(2), 316–335. https://doi.org/10.1111/j.1095-8312.2011.01681.x

Rabassa, J., & Coronota, A. (2009). Glaciations in Patagonia and Tierra del Fuego during the Ensenadan Stage/Age (Early Pleistocene–earliest Middle Pleistocene). *Quaternary International*, *210*(1-2), 18–36.

Ramasamy, R. K., Ramasamy, S., Bindroo, B. B., & Naik, V. G. (2014). STRUCTURE PLOT: A program for drawing elegant STRUCTURE bar plots in user friendly interface. *SpringerPlus*, *3*(1), 431. https://doi.org/10.1186/2193-1801-3-431

Rambaut, A. & Drummond, A. J. (2007). *Tracer v1.5*. http://beast.bio.ed.ac.uk/Tracer

Rangwala, S. H., Kuznetsov, A., Ananiev, V., Asztalos, A., Borodin, E., Evgeniev, V., Joukov, V., Lotov, V., Pannu, R., Rudnev, D., Shkeda, A., Weitz, E. M., & Schneider, V. A. (2021). Accessing NCBI data using the NCBI Sequence Viewer and Genome Data Viewer (GDV). *Genome Research*, *31*(1), 159–169. https://doi.org/10.1101/gr.266932.120

Rensch, B. (1929). *Das prinzip geographischer rassenkreise und das problem der artbildung*. Borntraeger.

Riesch, R., Muschick, M., Lindtke, D., Villoutreix, R., Comeault, A. A., Farkas, T. E., Lucek, K., Hellen, E., Soria-Carrasco, V., Dennis, S. R., de Carvalho, C. F., Safran, R. J., Sandoval, C. P., Feder, J., Gries, R., Crespi, B. J., Gries, G., Gompert, Z., & Nosil, P. (2017). Transitions between phases of genomic differentiation during stick-insect speciation. *Nature Ecology & Evolution*, *1*(4), 0082.

Rising, J.D. & Jaramillo, A. (2020). Rufous-collared Sparrow (*Zonotrichia capensis*), version 1.0. In J. del Hoyo, M. Elliott, D. A. C. Sargatal, & E. de Juana (Eds.), *Birds of the world*. Cornell Lab of Ornithology. https://doi.org/10.2173/bow.rucspa1.01

Rogalla, S., Patil, A., Dhinojwala, A., Shawkey, M. D., & D'Alba, L. (2021). Enhanced photothermal absorption in iridescent feathers. *Journal of the Royal Society Interface*, *18*(181), 20210252. https://doi.org/10.1098/rsif.2021.0252

Ronquist, F., Teslenko, M., van der Mark, P., Ayres, D. L., Darling, A., Höhna, S., Larget, B., Liu, L., Suchard, M. A., & Huelsenbeck, J. P.

(2012). MrBayes 3.2: Efficient Bayesian phylogenetic inference and model choice across a large model space. *Systematic Biology*, *61*(3), 539–542. https://doi.org/10.1093/sysbio/sys029

Sánchez, K. I., Recknagel, H., Elmer, K. R., Avila, L. J., & Morando, M. (2024). Tracing evolutionary trajectories in the presence of gene flow in South American temperate lizards (Squamata: *Liolaemus kingii* group). *Evolution*, *78*(4), 716–733. https://doi.org/10.1093/evolut/qpae009

Schubert, M., Lindgreen, S., & Orlando, L. (2016). AdapterRemoval v2: Rapid adapter trimming, identification, and read merging. *BMC Research Notes*, *9*(1), 1–7. https://doi.org/10.1186/s13104-016-1900-2

Sérsic, A. N., Cosacov, A., Cocucci, A. A., Johnson, L. A., Pozner, R., Avila, L. J., Sites Jr, J. W., & Morando, M. (2011). Emerging phylogeographical patterns of plants and terrestrial vertebrates from Patagonia. *Biological Journal of the Linnean Society*, *103*(2), 475–494. https://doi.org/10.1111/j.1095-8312.2011.01656.x

Stamatakis, A. (2014). RAxML version 8: A tool for phylogenetic analysis and post-analysis of large phylogenies. *Bioinformatics*, *30*(9), 1312–1313. https://doi.org/10.1093/bioinformatics/btu033

Tamura, K., Peterson, D., Peterson, N., Stecher, G., Nei, M., & Kumar, S. (2011). MEGA5: Molecular Evolutionary Genetics Analysis using maximum likelihood, evolutionary distance, and maximum parsimony methods. *Molecular Biology and Evolution*, *28*(10), 2731–2739. https://doi.org/10.1093/molbev/msr121

R team. (2018). *R Core Team. R: A language and environment for statistical computing*. R Foundation for Statistical Computing.

Turbek, S. P., Browne, M., Di Giacomo, A. S., Kopuchian, C., Hochachka, W. M., Estalles, C., Lijtmaer, D. A., Tubaro, P. L., Silveira, L. F., Lovette, I. J., Safran, R. J., Taylor, S. A., & Campagna, L. (2021). Rapid speciation via the evolution of pre-mating isolation in the Iberá Seedeater. *Science*, *371*(6536), eabc0256. https://doi.org/10.1126/science.abc0256

Turner, S. D. (2018). qqman: An R package for visualizing GWAS results using Q-Q and Manhattan plots. *Journal of Open Source Software*, *3*(25), 731. https://doi.org/10.21105/JOSS.00731

Tuttle, E. M., Bergland, A. O., Korody, M. L., Brewer, M. S., Newhouse, D. J., Minx, P., Stager, M., Betuel, A., Cheviron, Z. A., Warren, W. C., Gonser, R. A., & Balakrishnan, C. N. (2016). Divergence and functional degradation of a sex chromosome-like supergene. *Current Biology*, *26*(3), 344–350. https://doi.org/10.1016/j.cub.2015.11.069

Uy, J. A. C., Cooper, E. A., Cutie, S., Concannon, M. R., Poelstra, J. W., Moyle, R. G., & Filardi, C. E. (2016). Mutations in different pigmentation genes are associated with parallel melanism in island flycatchers. *Proceedings of the Royal Society B: Biological Sciences*, *283*(1834), 20160731. https://doi.org/10.1098/rspb.2016.0731

Uy, J. A. C., Irwin, D. E., & Webster, M. S. (2018). Behavioral isolation and incipient speciation in birds. *Annual Review of Ecology, Evolution, and Systematics*, *49*(1), 1–24. https://doi.org/10.1146/annurev-ecolsys-110617-062646

Wajahat, M., Bracken, C. P., & Orang, A. (2021). Emerging functions for snoRNAs and snoRNA-derived fragments. *International Journal of Molecular Sciences*, *22*(19), 10193. https://doi.org/10.3390/ijms221910193

Wang, S., Rohwer, S., de Zwaan, D. R., Toews, D. P. L., Lovette, I. J., Mackenzie, J., & Irwin, D. (2020). Selection on a small genomic region underpins differentiation in multiple color traits between two warbler species. *Evolution Letters*, *4*(6), 502–515. https://doi.org/10.1002/evl3.198

Weir, B. S., & Cockerham, C. C. (1984). Estimating *F*-statistics for the analysis of population structure. *Evolution*, *38*(6), 1358–1370. https://doi.org/10.1111/j.1558-5646.1984.tb05657.x

Weir, J. T., & Schluter, D. (2004). Ice sheets promote speciation in boreal birds. *Proceedings of the Royal Society B: Biological Sciences*, *271*(1551), 1881–1887. https://doi.org/10.1098/rspb.2004.2803

Weir, J. T., & Schluter, D. (2008). Calibrating the avian molecular clock. *Molecular Ecology*, *17*(10), 2321–2328. https://doi.org/10.1111/j.1365-294X.2008.03742.x

Winker, K. (2009). Reuniting phenotype and genotype in biodiversity research. *BioScience*, *59*(8), 657–665. https://doi.org/10.1525/bio.2009.59.8.7

Yoshimura, S., Gerondopoulos, A., Linford, A., Rigden, D. J., & Barr, F. A. (2010). Family-wide characterization of the DENN domain Rab GDP-GTP exchange factors. *The Journal of Cell Biology*, *191*(2), 367–381. https://doi.org/10.1083/jcb.201008051

Zamudio, K. R., Bell, R. C., & Mason, N. A. (2016). Phenotypes in phylogeography: Species' traits, environmental variation, and vertebrate diversification. *Proceedings of the National Academy of Sciences of the United States of America*, *113*(29), 8041–8048. https://doi.org/10.1073/pnas.1602237113

Zheng, X., Levine, D., Shen, J., Gogarten, S. M., Laurie, C., & Weir, B. S. (2012). A high-performance computing toolset for relatedness and principal component analysis of SNP data. *Bioinformatics*, *28*(24), 3326–3328. https://doi.org/10.1093/bioinformatics/bts606